16th European Signal Processing Conference (EUSIPCO 2008), Lausanne, Switzerland, August 25-29, 2008, copyright by EURASIP

VIRTUAL ERROR APPROACH TO NONLINEAR ADAPTIVE FILTERING FOR PARALLEL HAMMERSTEIN SYSTEMS

Tomohiro Ohno, and Akira Sano

Department of System Design Engineering, Keio University
3-14-1 Hiyoshi, Kohoku-ku, 223-8522 Yokohama, Japan
phone: + (81) 45 566 1730, fax: + (81) 45 566 1720, email: sano@sd.keio.ac.jp

ABSTRACT

A novel virtual error approach is proposed for fully adaptive feedforward compensation/equalization, which is useful in nonlinear active noise control and predistortion for nonlinear high power amplifier (HPA). To attenuate the compensation error, two kinds of virtual error are introduced and are forced into zero by adjusting three nonlinear adaptive filters in an on-line manner. It is shown that the convergence of the compensation error to zero can be assured by forcing the virtual errors to zero separately. The proposed method can adjust the predistorter directly without identification of a post-inverse model of HPA as adopted in previous predistortion methods. The effectiveness of the proposed virtual error approach is validated in numerical simulation with comparison to an ordinary nonlinear filtered-x algorithm in the adaptive predistortion for nonlinear HPA used in OFDM communication systems.

1. INTRODUCTION

Nonlinear adaptive feedforward compensation schemes have collected much attention in the areas of nonlinear active noise control and adaptive predistortion of nonlinear high power amplifiers (HPA). Fig. 1 shows a block diagram of an adaptive feedforward compensation in which the primary and secondary nonlinear path dynamics, $G(\cdot)$ and $H(\cdot)$ respectively, are uncertain or changeable. In a case of active noise control, the both primary and secondary path dynamics are uncertain and only $r(n)$, $u(n)$ and $e(n)$ are accessible, so the nonlinear filtered-x algorithm is applied along with the nonlinear system identification scheme for $G(\cdot)$ and $H(\cdot)$ [1]. In adaptive predistortion for HPA, the primary path dynamics $G(\cdot)$ is given, for instance, $G(\cdot) = z^{-L}$, so the predistorter is updated adaptively by adopting the nonlinear filtered-x algorithm with system identification to compensate the nonlinearity of HPA [2].

However, almost previous nonlinearity compensation schemes adopted an inverse modeling in which the HPA is followed by a post-inverse model which is updated the difference between the input to HPA and the output of inverse model is minimized, and then the predistorter is replaced by the updated inverse model at the front of the HPA [3][4][5][6][7]. These schemes are referred to as an indirect learning approach. On the other hand, the filtered-x algorithm can be regarded as a direct learning approach, since the preditorter is directly updated by using the compensation error $e(n)$ [2]. The direct approach can attain better performance due to robustness to noises and anticommutative property of the cascade of the HPA and the nonlinear post-inverse model [7]. However, the ordinary nonlinear filtered-x algorithm sometimes becomes unstable for a large step size in situation when there is an unknown dynamics $H(\cdot)$ between the adaptive predistorter $\hat{C}(\cdot)$ and the compensation error $e(n)$. Moreover, the nonlinear filtered-x algorithm was derived via some approximations in calculation of partial derivatives of the output $y(n)$ with respect to the compensator parameters.

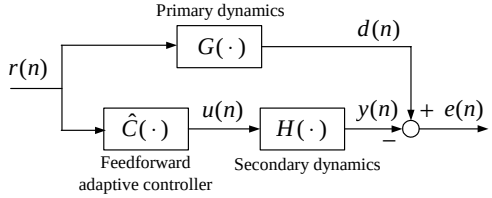

Figure 1: Adaptive feedforward compensation in case with uncertain nonlinear path dynamics

The purpose of this paper is to propose a novel direct learning approach which can directly tune the feedforward compensator (predistorter) $\hat{C}(\cdot)$ without identification of post-inverse model of HPA unlike the ordinary nonlinear filtered-x algorithm using the identified secondary path dynamics. To make the compensation error $e(n)$ zero, two virtual errors $e_A(n)$ and $e_B(n)$ are introduced (see Fig. 2) and are forced into zero by adjusting parameters in three nonlinear adaptive filters in an online manner. It is shown that the convergence of the compensation error to zero can be always attained if the filter parameters are adjusted and converge to any constants so that the two virtual errors can become zero. The proposed adaptive algorithm does not directly use the error $e(n)$ but the two virtual errors unlike the ordinary nonlinear filtered-x algorithm. The effectiveness of the proposed virtual error approach is clarified in comparison with ordinary nonlinear filtered-x algorithm in the adaptive predistortion for nonlinear HPA used in OFDM communication systems.

2. NONLINEAR ADAPTIVE FEEDFORWARD COMPENSATION PROBLEM

The schematic diagram in Fig. 1 illustrates an adaptive feedforward compensation system in which the primary and secondary nonlinear path dynamics, $G(\cdot)$ and $H(\cdot)$ are uncertain or changeable. The primary and secondary path dynamics are both unknown in nonlinear active noise control case, while only the secondary dynamics $H(\cdot)$ is uncertain in the predistortion for nonlinearity of HPA.

Assume that the primary and secondary path dynamics can be expressed by a parallel Hammerstein model (PHM)

or input polynomial series with memory (IPSM) as

$$d(n) = G(r(n)) = \sum_{m_1=0}^{M_1}\sum_{q_1=1}^{Q_1} g_{q_1,m_1}|r(n-m_1)|^{q_1-1}r(n-m_1) \quad (1)$$

$$y(n) = H(u(n)) = \sum_{m_2=0}^{M_2}\sum_{q_2=1}^{Q_2} h_{q_2,m_2}|u(n-m_2)|^{q_2-1}u(n-m_2) \quad (2)$$

where $q_1 = 1,3,5,\cdots,Q_1$ and $q_2 = 1,3,5,\cdots,Q_2$. The PHM has memoryless nonlinearity followed by linear dynamics which is used to express a class of nonlinear industrial processes [8].

In order to attenuate the compensation error $e(n)$ even in the presence of uncertainties in $\{g_{q_1,m_1}\}$ and $\{h_{q_2,m_2}\}$, an adaptive feedforward compensator $\hat{C}(\cdot)$ is employed. Its structure is also expressed similarly by an adaptive filer with PHM structure as

$$u(n) = C(r(n)) = \sum_{m_3=0}^{M_3}\sum_{q_3=1}^{Q_3} c_{q_3,m_3}|r(n-m_3)|^{q_3-1}r(n-m_3) \quad (3)$$

where $q_3 = 1,3,5,\cdots,Q_3$.

Now the problem is how to adjust the adaptive compensator parameters c_{q_3,m_3} by only using the accessible signals $r(n)$, $u(n)$ and $e(n)$ so that the compensation error $e(n)$ be forced to zero even if the nonlinear primary and secondary dynamics are unknown.

3. PROPOSED VIRTUAL ERROR APPROACH

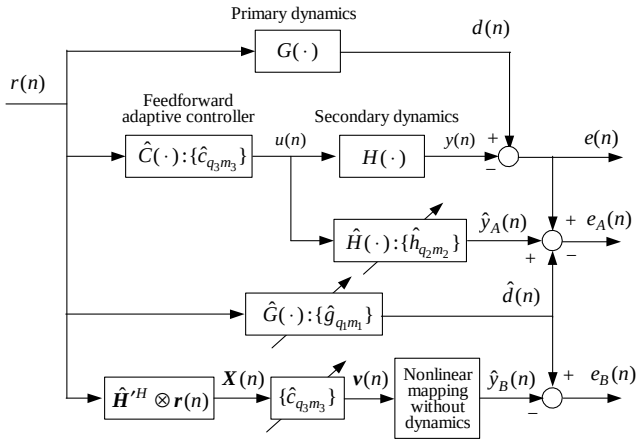

Figure 2: Proposed algorithm: Virtual error approach

Fig. 2 depicts the proposed virtual error algorithm in which three nonlinear adaptive filters are employed to force the canceling error $e(n)$ to zero. Two virtual errors $e_A(n)$ and $e_B(n)$ are also incorporated. The parameters $\{g_{q_1m_1}\}$ in $\hat{G}(\cdot)$ and $\{h_{q_2m_2}\}$ in $\hat{H}(\cdot)$ are updated to make the virtual error $e_A(n)$ zero, while the parameters $\{\hat{c}_{q_3,m_3}\}$ are updated to make $e_B(n)$ zero. In Section 5, it will be proved that the convergence of $e_A(N) \rightarrow 0$ and $e_B(N) \rightarrow 0$ results in the convergence of the compensation error $e(n)$ to zero.

Two kinds of virtual errors are now expressed, as shown in Fig. 2, by

$$e_A(n) = e(n) + \hat{y}_A(n) - \hat{d}(n) \quad (4)$$

$$e_B(n) = \hat{d}(n) - \hat{y}_B(n) \quad (5)$$

The parameters $\{\hat{g}_{q_1m_1}\}$ and $\{\hat{h}_{q_2m_2}\}$ in the primary and secondary path dynamics are now updated so as to let the virtual error $e_A(n)$ zero. The adaptive feedforward compensator and the predicted outputs $\hat{y}_A(n)$ and $\hat{d}(n)$ are expressed as

$$u(n) = \hat{\boldsymbol{c}}^H(n')\boldsymbol{r}(n) \quad (6)$$

$$\hat{y}_A(n) = \hat{\boldsymbol{h}}^H(n')\boldsymbol{u}(n) \quad (7)$$

$$\hat{d}(n) = \hat{\boldsymbol{g}}^H(n')\boldsymbol{r}(n) \quad (8)$$

where

$$\begin{aligned}
\boldsymbol{r}(n) &= [r(n),|r(n)|^2r(n),\cdots,|r(n)|^{Q_3-1}r(n),r(n-1),\\
&\quad |r(n-1)|^2r(n-1),\cdots,|r(n-1)|^{Q_3-1}r(n-1),r(n-M_3),\\
&\quad |r(n-M_3)|^2r(n-M_3),\cdots,|r(n-M_3)|^{Q_3-1}r(n-M_3)]^T\\
\hat{\boldsymbol{c}}^*(n') &= [\hat{c}_{10}(n'),\hat{c}_{30}(n')\cdots,\hat{c}_{Q_30}(n'),\hat{c}_{11}(n'),\hat{c}_{31}(n'),\\
&\quad \cdots,\hat{c}_{Q_31}(n'),\cdots,\hat{c}_{1M_3}(n'),\hat{c}_{3M_3}(n'),\cdots,\hat{c}_{Q_3M_3}(n')]^T\\
\boldsymbol{u}(n) &= [u(n),|u(n)|^2u(n),\cdots,|u(n)|^{Q_2-1}u(n),u(n-1),\\
&\quad |u(n-1)|^2u(n-1),\cdots,|u(n-1)|^{Q_2-1}u(n-1),u(n-M_2),\\
&\quad |u(n-M_2)|^2u(n-M_2),\cdots,|u(n-M_2)|^{Q_2-1}u(n-M_2)]^T\\
\hat{\boldsymbol{h}}^*(n') &= [\hat{h}_{10}(n'),\hat{h}_{30}(n'),\cdots,\hat{h}_{Q_20}(n'),\hat{h}_{11}(n'),\hat{h}_{31}(n'),\\
&\quad \cdots,\hat{h}_{Q_21}(n'),\cdots,\hat{h}_{1M_2}(n'),\hat{h}_{3M_2}(n'),\cdots,\hat{h}_{Q_2M_2}(n')]^T\\
\hat{\boldsymbol{g}}^*(n') &= [\hat{g}_{10}(n'),\hat{g}_{30}(n'),\cdots,\hat{g}_{Q_10}(n'),\hat{g}_{11}(n'),\hat{g}_{31}(n'),\\
&\quad \cdots,\hat{g}_{Q_11}(n'),\cdots,\hat{g}_{1M_1}(n'),\hat{g}_{3M_1}(n'),\cdots,\hat{g}_{Q_1M_1}(n')]^T
\end{aligned}$$

On the other hand, $\hat{y}_B(n)$ is also needed to obtain an explicit form of the virtual error $e_B(n)$. For the purpose, we introduce the intermediate signal matrix as

$$\begin{aligned}
\boldsymbol{X}(n) &= [\hat{h}'_{10},\hat{h}'_{30}\cdots,\hat{h}'_{Q_20},\cdots,\hat{h}'_{1M_2},\hat{h}'_{3M_2},\cdots,\hat{h}'_{Q_2M_2}]\\
&\quad \otimes \begin{bmatrix} r(n)\\ |r(n)|^2r(n)\\ \vdots\\ |r(n)|^{Q-1}r(n)\\ \vdots\\ r(n-M_3)\\ |r(n-M_3)|^2r(n-M_3)\\ \vdots\\ |r(n-M_3)|^{Q_2-1}r(n-M_3)\end{bmatrix}\\
&\equiv [\boldsymbol{x}_{10}(n),\boldsymbol{x}_{30}(n),\cdots,\boldsymbol{x}_{Q_20}(n),\cdots,\\
&\quad \boldsymbol{x}_{1M_2}(n),\boldsymbol{x}_{3M_2}(n),\cdots,\boldsymbol{x}_{Q_2M_2}(n)]
\end{aligned} \quad (9)$$

where $\otimes$ is the Kronecker product, and $\hat{h}'_{qm}$ is denoted by

$$\hat{h}'_{qm} = |\hat{h}_{qm}|^{1/q}\exp(j\angle\hat{h}_{qm}) \quad (10)$$

By using the above signal matrix, we introduce another signal vector $\boldsymbol{v}(n)$ defined as

$$\boldsymbol{v}^T(n) = [\hat{c}_{10}(n'),\hat{c}_{30}(n'),\cdots,\hat{c}_{Q_20}(n'),\cdots,$$

$$\hat{c}_{1,M_2}(n'),\hat{c}_{3,M_2}(n'),\cdots,\hat{c}_{Q_2M_2}]$$
$$\cdot[\boldsymbol{x}_{10}(n),\boldsymbol{x}_{30}(n)\cdots,\boldsymbol{x}_{Q_20}(n),\cdots,\boldsymbol{x}_{1M_2}(n-M_2),$$
$$\boldsymbol{x}_{3M_2}(n-M_2),\cdots,\boldsymbol{x}_{Q_2M_2}(n-M_2)]$$
$$\equiv[v_{10}(n),v_{30}(n),\cdots,v_{Q_20}(n),\cdots,$$
$$v_{1M_2}(n),v_{3M_2}(n),\cdots,v_{Q_2M_2}(n)] \quad (11)$$

Thus, we can express the predicted output $y_B(n)$ by a *nonlinear mapping without dynamics* using the signal vectors defined above, as

$$\begin{aligned}\hat{y}_B(n) &= v_{10}(n)+|v_{30}(n)|^2v_{30}(n)+\cdots\\ &+|v_{Q_20}(n)|^{Q_2-1}v_{Q_20}(n)+v_{11}(n)+|v_{31}(n)|^2v_{31}(n)\\ &+\cdots+|v_{Q_21}(n)|^{Q_2-1}v_{Q_21}(n)\\ &\vdots\\ &+v_{1M_2}(n)+|v_{3M_2}(n)|^2v_{3M_2}(n)+\cdots\\ &+|v_{Q_21}(n)|^{Q_2-1}v_{Q_2M_2}(n)\end{aligned} \quad (12)$$

It should be noticed that there is no dynamics between the adaptive filter $\{\hat{c}_{q_3m_3}\}$ and the virtual error $e_B(n)$, that is different from the ordinary nonlinear filtered-x algorithm and it will make the propsed method highly robust.

4. ADAPTIVE ALGORITHM

The error system for the virtual error $e_A(n)$ is expressed by using the notation defined in the previous section as

$$e_A(n)=e(n)+\hat{\boldsymbol{h}}^H(n)\boldsymbol{u}(n)-\hat{\boldsymbol{g}}^H(n)\boldsymbol{r}(n) \quad (13)$$

Then, the adjustable parameters are updated by a normalized LMS algorithm as

$$\hat{\boldsymbol{h}}(n)=\hat{\boldsymbol{h}}(n-1)-\gamma_h\boldsymbol{u}(n)\varepsilon_A(n) \quad (14)$$
$$\hat{\boldsymbol{g}}(n)=\hat{\boldsymbol{g}}(n-1)+\gamma_h\boldsymbol{r}(n)\varepsilon_A(n) \quad (15)$$
$$\varepsilon_A(n)=\frac{e_A(n)}{1+\gamma_h\|\boldsymbol{u}(n)\|^2+\gamma_g\|\boldsymbol{r}(n)\|^2}$$

The other virtual error $e_B(n)$ is given by

$$e_B(n)=\hat{d}(n)-\hat{y}_B(n)$$

where $\hat{y}_B(n)$ is given by (5), (8), (9), (11) and (12) as a function of the parameters $\{\hat{c}_{q_3m_3}\}$. The parameters are updated by a normalized LMS algorithm as

$$\hat{\boldsymbol{c}}(n)=\hat{\boldsymbol{c}}(n-1)-\gamma_c(\varepsilon_B^*(n)\boldsymbol{\varphi}(n)+\varepsilon_B(n)\boldsymbol{\psi}(n)) \quad (16)$$

where

$$\begin{aligned}\boldsymbol{\varphi}(n) &= [\boldsymbol{x}_{10}(n)+2|v_{30}(n)|^2\boldsymbol{x}_{30}(n)+\cdots\\ &+(Q_2+1)/2\,|v_{Q_20}(n)|^{Q_2-1}\boldsymbol{x}_{Q_20}(n)\cdots\\ &+\boldsymbol{x}_{1M_2}(n-M_2)+2|v_{3M_2}(n)|^2\boldsymbol{x}_{3M_2}(n-M_2)+\cdots\\ &+(Q_2+1)/2\,|v_{Q_2M_2}|^{Q_2-1}(n)\boldsymbol{x}_{Q_2M_2}(n-M_2)]^T\\ \boldsymbol{\psi}(n) &= [v^{*2}_{30}(n)\boldsymbol{x}_{30}(n)+2|v_{50}(n)|^2v^{*2}_{50}\boldsymbol{x}_{50}(n)+\cdots\\ &+(Q_2-1)/2\,|v_{Q_20}(n)|v^{*2}_{Q_20}(n)\boldsymbol{x}_{Q_20}(n)+\cdots\\ &+v^{*2}_{3M_2}(n)\boldsymbol{x}_{3M_2}(n-M_2)\\ &+2|v_{5M_2}|^2v^*\,2_{5M_2}(n)\boldsymbol{x}_{5M2}(n-M_2)+\cdots\\ &+(Q_2-1)/2\,|v_{Q_2M_2}(n)|^{Q_2-3}v^{*2}_{Q_2M_2}\boldsymbol{x}_{Q_2M_2}(n-M_2)]^T\end{aligned}$$
$$\varepsilon_B(n)=\frac{e_B(n)}{1+\gamma_c(\|\boldsymbol{\varphi}(n)\|^2+\|\boldsymbol{\psi}(n)\|^2)} \quad (17)$$

5. PROPERTY OF VIRTUAL ERROR APPROACH

In the section, we will clarify why the compensation error $e(n)$ converges to zero if the parameters of the three adaptive filters converge to any constants so that the two virtual errors $e_A(n)$ and $e_B(n)$ converge to zero separately.

We consider the sum of two virtual errors $e_A(n)$ and $e_B(n)$, and then it follows from (4) and (5) that

$$e_A(n)+e_B(n)=e(n)+\hat{y}_A(n)-\hat{y}_B(n) \quad (18)$$

Now we can show that the compensation error $e(n)$ converges to zero, if the parameters in the three nonlinear adaptive filters in Fig.2 can be updated so that the errors $e_A(n)$ and $e_B(n)$ may become zero, and these filter parameters converge to any constant values. To prove this property, we should show that

$$\hat{y}_A(n)=\hat{y}_B(n) \quad (19)$$

for sufficiently large n.

For the simplicity, the proof is done in a case with $Q_2=3$ and $M_2=1$. We introduce the notation of some operators which will make manipulations very simple.

$$\begin{aligned}N_q\{\cdot\} &= |\{\cdot\}|^{q-1}\{\cdot\}\\ \hat{C}\{\cdot\} &= [\hat{c}_{10}+\hat{c}_{30}N_3+\cdots+\hat{c}_{Q_20}N_{Q_2}\\ &+\hat{c}_{11}z^{-1}+\hat{c}_{31}N_3z^{-1}+\cdots+\hat{c}_{Q_21}N_{Q_2}z^{-1}\\ &\vdots\\ &+\hat{c}_{1M_2}z^{-M_2}+\hat{c}_{3M_2}N_3z^{-M_2}+\cdots+\hat{c}_{Q_2M_2}N_{Q_2}z^{-M_2}]\{\cdot\}\\ \hat{H}\{\cdot\} &= [\hat{h}_{10}+\hat{h}_{30}N_3+\cdots+\hat{h}_{Q_20}N_{Q_2}\\ &+\hat{h}_{11}z^{-1}+\hat{h}_{31}N_3z^{-1}+\cdots+\hat{h}_{Q_21}N_{Q_2}z^{-1}\\ &\vdots\\ &+\hat{h}_{1M_2}z^{-M_2}+\hat{h}_{3M_2}N_3z^{-M_2}+\cdots+\hat{h}_{Q_2M_2}N_{Q_2}z^{-M_2}]\{\cdot\}\end{aligned}$$

Then by using the above operators, the predicted output $\hat{y}_A(n)$ can be expressed by

$$\begin{aligned}\hat{y}_A(n) &= \hat{H}\{\hat{C}\{r(n)\}\}\\ &= [\hat{h}_{10}+\hat{h}_{30}N_3+\hat{h}_{11}z^{-1}+\hat{h}_{31}N_3z^{-1}]\\ &\quad[\hat{c}_{10}+\hat{c}_{30}N_3+\hat{c}_{11}z^{-1}+\hat{c}_{31}N_3z^{-1}]\{r(n)\}\\ &= \hat{h}_{10}[\hat{c}_{10}+\hat{c}_{30}N_3+\hat{c}_{11}z^{-1}+\hat{c}_{31}N_3z^{-1}]\{r(n)\}\\ &+\hat{h}_{30}N_3\{[\hat{c}_{10}+\hat{c}_{30}N_3+\hat{c}_{11}z^{-1}+\hat{c}_{31}N_3z^{-1}]\{r(n)\}\}\\ &+\hat{h}_{11}z^{-1}\{[\hat{c}_{10}+\hat{c}_{30}N_3+\hat{c}_{11}z^{-1}+\hat{c}_{31}N_3z^{-1}]\{r(n)\}\}\\ &+\hat{h}_{31}N_3\{[\hat{c}_{10}+\hat{c}_{30}N_3+\hat{c}_{11}z^{-1}+\hat{c}_{31}N_3z^{-1}]\{r(n)\}\}\end{aligned} \quad (20)$$

On the other hand, the predicted output $\hat{y}_B(n)$ can also be expressed by using the notations of operators as

$$\begin{aligned}\hat{y}_B(n) &= [\hat{c}_{10}\hat{h}'_{10}+\hat{c}_{30}\hat{h}'_{10}N_3+\hat{c}_{11}\hat{h}'_{10}z^{-1}\\ &\quad+\hat{c}_{31}\hat{h}'_{10}N_3z^{-1}]\{r(n)\}\\ &+N_3\{[\hat{c}_{10}\hat{h}'_{30}+\hat{c}30\hat{h}'_{30}N_3+\hat{c}_{11}\hat{h}'_{30}z^{-1}\\ &\quad+\hat{c}_{31}\hat{h}'_{30}N_3z^{-1}]\{r(n)\}\\ &+[\hat{c}_{10}z^{-1}\hat{h}'_{11}+\hat{c}_{30}z^{-1}\hat{h}'_{11}N_3+\hat{c}_{11}z^{-1}\hat{h}'_{11}z^{-1}\end{aligned}$$

$$+\hat{c}_{31}z{-}1\hat{h}'_{11}N_3z^{-1}]\{r(n)\}$$
$$+N_3\{\{[\hat{c}_{10}z^{-1}\hat{h}'_{31}+\hat{c}_{30}z^{-1}\hat{h}'_{31}N_3+\hat{c}_{11}z^{-1}\hat{h}'_{31}z^{-1}$$
$$+\hat{c}_{31}z^{-1}\hat{h}'_{31}z^{-1}]\{r(n)\}\} \tag{21}$$

If all the adjustable parameters $\hat{g}_{qm}(n)$, $\hat{h}_{qm}(n)$ and $\hat{c}_{qm}(n)$ are updated by the adaptive algorithms in (14), (15) and (16) so that $e_A(n)\to 0$ and $e_B(n)\to 0$ can be attained, and these parameters converge to any constants $\bar{g}_{qm}$, $\bar{h}_{qm}$ and $\bar{c}_{qm}$, we can apply the following commutative properties as

$$\bar{h}'_{qm}z^{-1}x(n)=z^{-1}\bar{h}'_{qm}x(n)$$
$$\bar{c}_{qm}z^{-1}x(n)=z^{-1}\bar{c}'_{qm}x(n)$$
$$\bar{c}_{qm}\bar{h}'_{qm}x(n)=\bar{h}'_{qm}\bar{c}_{qm}x(n)$$
$$\bar{h}_{qm}N_q\{x(n)\}=N_q\{\bar{h}'_{qm}x(n)\}$$

Then it follows from (20) and (21) that

$$\hat{y}_A(n)=\hat{y}_B(n)\quad \text{for } n\to\infty \tag{22}$$

Then we can conclude that

$$e(n)=e_A(n)+e_B(n)=y_A(n)-y_B(n)\to 0 \tag{23}$$

6. APPLICATION TO ADAPTIVE PREDISTORTION FOR NONLINEAR HPA

The proposed algorithm is applied to adaptive predistortion for nonlinear HPA in 64 QAM OFDM transmission system. The baseband OFDM signal is described by

$$\begin{aligned} s(n\Delta T) &= \sum_{k=-N/2}^{N/2-1} c_k e^{(j2\pi k f_0 n\Delta T)} \\ &= s_I(n\Delta T)+js_Q(n\Delta T) \end{aligned} \tag{24}$$

The simulation setup is summarized as follows: The transmitted symbol $c_k=\alpha_k+j\beta_k$ is 64 QAM OFDM signal which takes discrete values as α_k, $\beta_k\in\{\pm1,\pm3,\pm5,\pm7\}$, the size of FFT is 2048, and the number of subcarriers is 400. The guard interval is 1024, and the total number of data is $(2048+1024)\times 6$ for evaluation of the proposed method.

It is assumed in the simulation that the true nonlinear HPA is characterized by modifying the Saleh model [9] as

$$x(n)=[0.7,0.2]\begin{bmatrix} u(n)\\ u(n-1)\end{bmatrix}$$
$$y(n)=A(|u(n)|)e^{j\{\angle u(n)+P(|u(n)|)\}}$$
$$A(|u(n)|)=a\times\frac{2|u(n)|}{1+|u(n)|^2}$$
$$P(|u(n)|)=a\times\frac{\pi}{3}\left\{\frac{|u(n)|^2}{1+|u(n)|^2}\right\}$$
$$a=2,4,6,8,10$$

Fig. 3 shows an input-output property of HPA, which is given by AM/AM and PM/AM properties. In order to evaluate the tracking performance of the proposed virtual error approach, we changed the value of a from $a=1$ to various values $a=2\sim 10$ at the sampling instant 5000. The model orders of the HPA and the predistorter are set to $Q_2=Q_3=5$, and $M_2=M_3=2$. The purpose of the simulation is to clarify the effectiveness of the proposed virtual error approach in comparison with a normalized nonlinear filtered-x algorithm in the tracking and detection performance. The tracking performance is evaluated by the time average of the compensation errors $\bar{e^2}$, and the detection performance is also given by

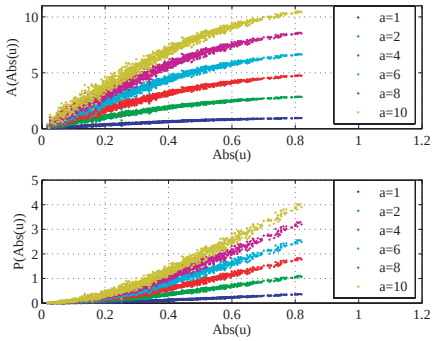

Figure 3: Input-output property in amplitude and phase of nonlinear HPA

$$\text{EVM}=\sqrt{\frac{\sum_{n=1}^{N}|c_n-d_n|^2}{\sum_{n=1}^{N}|c_n|^2}} \tag{25}$$

where c_n is a transmitted symbol and d_n is a detected symbol corresponding to c_n.

FIg. 4 and Fig. 5 summarize the profiles of the updated parameters $\{\hat{h}_{q_2m_2}\}$ of the HPA model, $\{\hat{c}_{q_3m_3}\}$ of the predistorter and the compensation error $e(n)$ with the virtual errors $e_A(n)$ and $e_B(n)$, in comparison with the filtered-x algorithm and the proposed virtual error approach. Table 1 also shows the comparison of the tracking and detection performances.

It can be seen in Figs. 4 and 5 that the proposed approach is more robust to changes of the HPA dynamics and the filtered-x algorithm becomes unstable in case with $a=10$. It is also shown that the convergence of the virtual errors $e_A(n)\to 0$ and $e_B(n)\to 0$ is established and then the convergence of the compensation error $e(n)\to 0$ is also obtained as a result. The nonlinear filtered-x algorithm adopts some approximation in the calculation of partial derivatives of the HPA output with respect to the weight parameters $\hat{c}_{q_3m_3}\}$

Table 1: Comparison of performances between Filtered-x algorithm and proposed virtual error approach

a	Filtered-x algorithm		Virtual error method	
	$\lvert e\rvert^2$	EVM	$\lvert e\rvert^2$	EVM
2	3.43×10^{-3}	6.94×10^{-2}	8.07×10^{-4}	3.87×10^{-2}
4	5.17×10^{-3}	1.26×10^{-1}	1.70×10^{-3}	8.34×10^{-2}
6	8.47×10^{-3}	1.94×10^{-1}	3.48×10^{-3}	1.33×10^{-1}
8	1.56×10^{-2}	2.99×10^{-1}	6.03×10^{-3}	1.82×10^{-1}
10	1.36×10^{1}	9.07	9.20×10^{-3}	2.29×10^{-1}

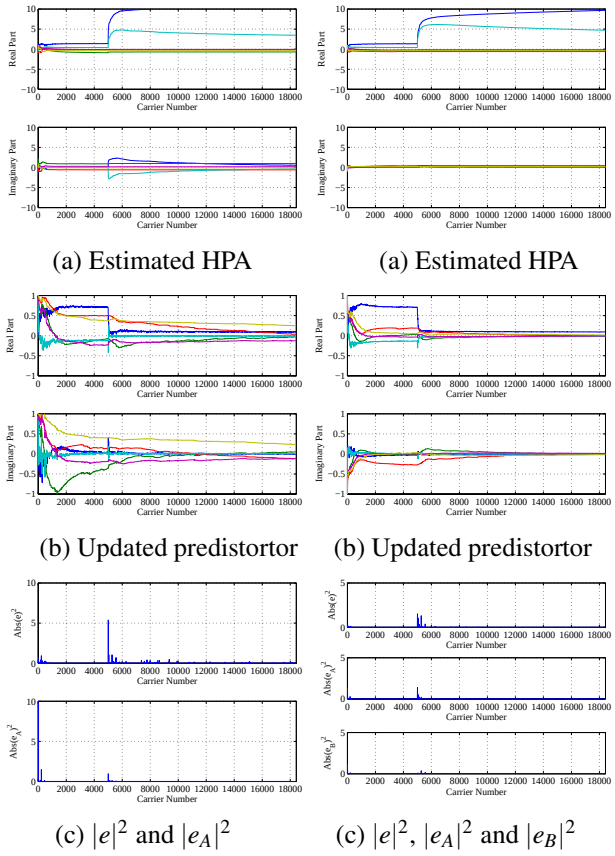

Figure 4: Comparison of Filtered-x algorithm (*Left*) and proposed virtual error approach (*Right*) in case with $a = 8$

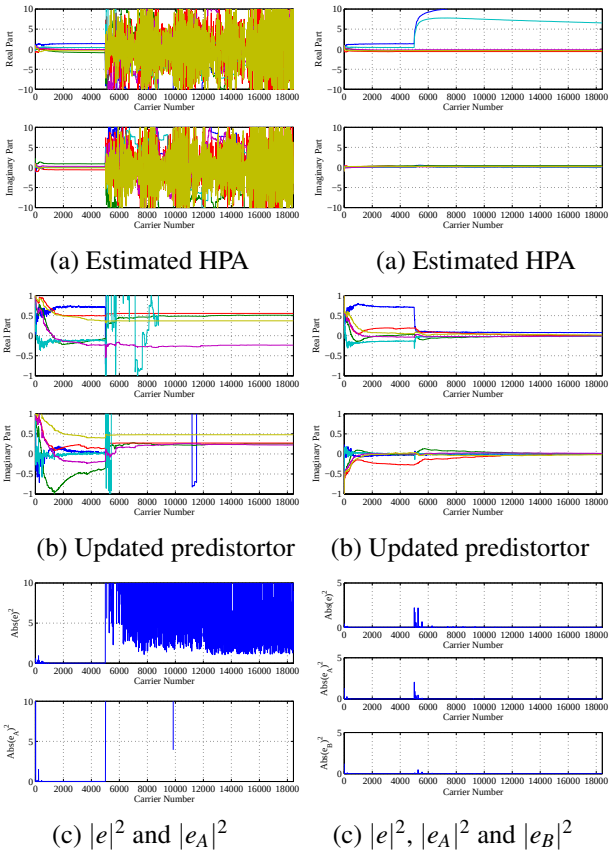

Figure 5: Comparison of Filtered-x algorithm (*Left*) and proposed virtual error approach (*Right*) in case with $a = 10$

in derivation of the algorithm, while the proposed approach does not use any approximation, that is one of the reasons why the proposed virtual error approach has fast convergence and robust stability.

7. CONCLUSION

We have presented the new direct adaptive algorithm for tuning the feedforward controller, which can work in stable manner even when the nonlinear primary and secondary path dynamics are uncertain. It is shown that the convergence of two virtual errors to zero can guaranteed the convergence of the compensation error. The effectiveness of the proposed virtual error approach was clarified in the application of the adaptive predistortion for nonlinear HPA.

REFERENCES

[1] Y. H. Lim, Y. S. Cho, I. W. Cha and D. H. Youn, "An adaptive nonlinear prefilter for compensation of distortion in nonlinear systems," *IEEE Trans. Signal Processing*, vol. 46, pp. 1726–1730, June 1998.

[2] D. Zhou and V. E. DeBeunner, "Novel adaptive nonlinear predistorters based on the direct learning algorithm," *IEEE Trans. Signal Processing*, vol. 55, pp. 120–133, Jan. 2007.

[3] L. Sun, Y. Ding and A. Sano, "Identification-based predistortion scheme for high power amplifier," *IEICE Trans. Fundamentals*, vol. E86-A, pp. 874–881, April 2003.

[4] H. Ku and J .S. Kenney, "Behavioral modeling of nonlinear RF power amplifiers considering memory effects," *IEEE Trans. Microwave Theory and Tech.*, vol. 51, pp. 2495–2504, Dec. 2003.

[5] J. C. Pedro and S. A. Mass, "A comparative overview of microwave and wireless power-amplifier behavioral modeling approaches," *IEEE Trans. Microwave Theory and Tech.*, vol. 53, pp. 1150–1163, April 2005.

[6] M. Isaksson, D. W. Wisell and D. R. Ronnow, "A comparative analysis of behavioral models for RF power amplifier," *IEEE Trans. Microwave Theory and Tech.*, vol. 54, pp. 348–359, Jan. 2006.

[7] D. R. Morgan, Z. Ma, J. Kim, M. G. Zierdt and J. Pastalan, "A generalized memory polynomial model for digital predistortion of RF power amplifiers," *IEEE Trans. Signal Processing*, vol. 54, pp. 3852–3860, Oct. 2006.

[8] J. Wang, A. Sano, D. Shook, T. Chen and B. Huang, "A blind approach to closed-loop identification of Hammerstein systems", *Int. J. Control*, vol. 80, no. 2, pp. 302–313, 2007.

[9] A. A. M. Saleh and J. Salz, "Adaptive linearization of power amplifiers in digital radio systems", *The Bell Sys. Tech. J.*, Vol. 62, No. 4, pp. 1019–1034, 1983.